International Journal of Soft Computing and Engineering (IJSCE)
ISSN: 2231-2307, Volume-2, Issue-1, March 2012

Fall Detection for the Elderly using a Support Vector Machine

Patimakorn Jantaraprim, Pornchai Phukpattaranont, Chusak Limsakul, Booncharoen Wongkittisuksa

***Abstract*— We propose a short time min-max feature for improving fall detection performance based on the specific signatures of critical phase fall signal, acquired using a tri-axial accelerometer on a torso. Our proposed feature has been validated by a Support Vector Machine with two-fold cross-validation. Fall and scripted activities were tested in the experiment. Performance was evaluated by comparing the short time min-max with a maximum peak feature. The results obtained from 420 sequences show that the performances of short time min-max feature can approach 98.2% sensitivity and 100% specificity for a radial basis function kernel, which are better than those from the maximum peak feature for all testing kernels. The short time min-max feature also uses one sensor for the body's position without a fixed threshold for 100% sensitivity or specificity, and without additional processing of a posture after a fall. The simplicity and high performance of our proposed feature makes it suitable for implementation on a microcontroller for use in practical situations.**

***Index Terms*— Fall detection, Critical phase, Short time min-max feature, Support Vector Machine.**

I. INTRODUCTION

The number of elderly (i.e. people aged over 60 years) is estimated to reach almost two billion by 2050 [1]. One major public health problems for the elderly are falls and consequential injures, which will only get worse as the numbers of elderly increases. Major causes for fall-related hospital admissions are hip fractures, traumatic brain injuries, and upper limb injuries, resulting in a significant increase in the health care costs [2]. For example, the average cost of hospitalization for fall-related injuries for people aged 65 years and older range from US$ 6,646 in Ireland to US$ 17,483 in the USA [3, 4]. However, if the elderly could get help as soon as possible after the fall, the severity of the injury could be reduced. Also, it results in decreasing the risk of paralysis, the rate of sickness, death and the medical cost.

Image processing and sensors are two most popular techniques for fall detection [5]. Image processing performs very well [6]-[9] in controlled environments for the lighting and frame. Also, sensor methods are promising [10]-[18]. Nine micro mercury switches and an optical sensor attached to ten places around a coat were used for Lin's study [10]. By his fall after impact detection, the results show sensitivities of 98-100%. Using a tri-axial accelerometer attached to the waist or head for Kangas' study [11], two or more phases of a fall event were employed: the beginning of the fall, falling velocity, fall impact, and subsequent posture of the person. Using a simple threshold with three different detection algorithms (impact + posture, start of fall + impact + posture, and start of fall + velocity + impact + posture), his study reported 97-98% sensitivity and 100% specificity (by setting thresholds) for three middle aged subjects. The same algorithms with more subjects were investigated in his recent study, which obtain a sensitivity of 97.5% and a specificity of 100% (by setting thresholds) [12]. A tri-axial accelerometer was also employed by Chao's study [13]. A cross-product (AC) was proposed as a parameter, and compared to the acceleration magnitude (AM). AC leads to a larger area under a receiver operating characteristic curve than AM. Moreover, including post-fall posture (PP) recruitment leads to lower false alarm ratios for both AC- and AM-based methods. Sitting-to-lying motion was reported to produce false alarms in his study. A biaxial gyroscope, a tri-axial accelerometer, and an inertial sensor (a tri-axial + a gyroscope) were employed for Bourke's studies [14]-[16]. He reported 100% sensitivity (by setting thresholds) and 100% specificity using a threshold-based algorithm. However, our study [17] with the same algorithm used in Bourke's study [15] found that some false positives occur for quick movements. This was confirmed in his recent work with scripted and unscripted activities [16], which utilized thresholds for velocity, impact, and posture to achieve 100% sensitivity (by setting thresholds) and 100% specificity. His study [16] needs signals from both an accelerometer and a gyroscope to find the velocity.

Addition of posture after a fall [11]-[12], post-fall posture recruitment [13] and posture after a fall [16] are needed to improve their fall detection performance. Moreover, some studies need fixed thresholds, which are obtained from the experiment, for 100% sensitivity or specificity.

A fall can be described as the rapid change from the upright/sitting position to the reclining or almost lengthened position, but is an uncontrolled movement. A fall has been defined to have four distinct phases [5]:

(1) Pre-fall phase, comprising usual/normal activities of daily living (ADL), but may contain some instability;

Manuscript received Dec 29, 2011.

Patimakorn Jantaraprim, Department of Electrical Engineering, Faculty of Engineering, Prince of Songkla University, Hat Yai, Songkhla, Thailand, 90112, +66 74 212894, (e-mail: patimakorn.j@hyac.in.th).

Pornchai Phukpattaranont, Department of Electrical Engineering, Faculty of Engineering, Prince of Songkla University, Hat Yai, Songkhla, Thailand, 90112, +66 74 212894, (e-mail: pornchai.p@psu.ac.th).

Chusak Limsakul, Department of Electrical Engineering, Faculty of Engineering, Prince of Songkla University, Hat Yai, Songkhla, Thailand, 90112, +66 74 212894, (e-mail: chusak.l@psu.ac.th).

Booncharoen Wongkittisuksa, Department of Electrical Engineering, Faculty of Engineering, Prince of Songkla University, Hat Yai, Songkhla, Thailand, 90112, +66 74 212894, (e-mail: booncharoen.w@psu.ac.th).

(2) Critical phase, when the body experiences a sudden movement towards the ground, ending with a vertical shock;

(3) Post-fall phase, when the body remains inactive, frequently lying on the ground;

(4) Recovery phase, when the person stands up on his own, or with the help of others.

During a critical phase fall, the body moves suddenly towards the ground, ending with a vertical shock. Therefore, a resultant from 3-axis acceleration, here the resultant acceleration of a torso is suddenly changed to a high negative and a positive peak in a short time interval. The high negative occurs when the body moves suddenly towards the ground. The high positive occurs when the body contacts the ground.

This article proposes a short time min-max feature for fall detection. This feature employs specific characteristics of high negative and positive resultant acceleration peaks in short time, which occurs during critical phase fall signals. This feature distinguishes falls from ADL, that usually have a low negative and/or positive resultant acceleration peaks. The aims of this study are

(1) to show that the minimum and maximum resultant accelerations observed during a critical phase fall of a torso can distinguish falls from ADL using a Support Vector Machine, without a fixed threshold for 100% sensitivity or specificity,

(2) to propose a short time min-max feature, which is evaluated from the minimum and maximum resultant accelerations in a defined window for fall detection, and

(3) to compare performances for a short time min-max and a maximum peak feature and show that the short time min-max feature can approach the better performance.

The rest of this article is organized as follows: Section 2 describes materials and methods, Section 3 presents results, Section 4 contains discussion, and conclusions are given in Section 5.

II. Materials and Methods

A. Materials

As in our previous study [18], a tri-axial accelerometer was constructed using two dual-axis MEMS accelerometers (Analog Devices ADXL321) mounted at right angles to each other, and attached to a person's torso as shown in Figure 1. The X axis is anterior-posterior, the Y axis is left-right, and the Z axis is superior-inferior. Signals from each axis were transmitted by wires connected to each accelerometer, transformed from analog to digital by NI-USB6008, and recorded for later offline processing. All signals were acquired at 12-bit resolution with a 1-kHz sampling frequency, and processed by a second-order low-pass Butterworth digital filter with a cut-off frequency of 20 Hz. The trial protocols were approved by the Research Ethics Committee of the Electrical Engineering Department of Prince of Songkla University. Written informed consents were obtained from all subjects prior to the experiments.

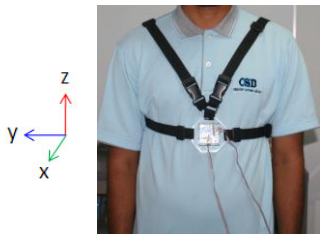

Figure 1: Position of the tri-axial accelerometer.

B. Fall and ADL Experiments

Data from our previous study [18] were used, and added more subjects. A predefined set of falls and ADL common to the elderly were evaluated for performance. Young subjects were performed simulated falls onto a mattress for safety and health concerns. 14 young and 14 elderly subjects were involved in the experiments (7 male and 7 female for young, age 25.14 ± 5.26 years, 7 male and 7 female for elderly, age 68.28 ± 4.37 years). Four categories of fall: forward fall (FF), backward fall (BF), left side fall (LF), and right side fall (RF), and six categories of ADL: sit-stand (ST), stand-sit (TS), sit-lie on a bed/floor (SL), lie-sit (LS), bend down to pick up an object when standing (BD), and walk (WA) were performed. Each fall and ADL type was repeated three times for each subject, so the data comprised 420 sequences, made up from 168 fall and 252 ADL sequences.

C. Features

Resultant acceleration (A_{res}) can be evaluated from the representatives of the 3-axis acceleration. If A_x, A_y, and A_z are accelerations (g) along the x, y, and z axes, then the resultant acceleration can be expressed as:

$$A_{res} = \sqrt{(A_x)^2 + (A_y)^2 + (A_z)^2} \qquad (1)$$

An example of a left side fall signal, displayed in terms of x, y, and z accelerations is shown in Figure 2a, while the resultant acceleration corresponding to Figure 2a is shown in Figure 2b. Two features, a maximum peak and a short time min-max feature were tested in the experiment.

Maximum peak feature

A fall produces high resultant acceleration as impact, so a maximum resultant acceleration peak, $\max(A_{res})$, was used as a feature for a fall. Figure 2c shows $\max(A_{res})$ of the example of left side fall signal.

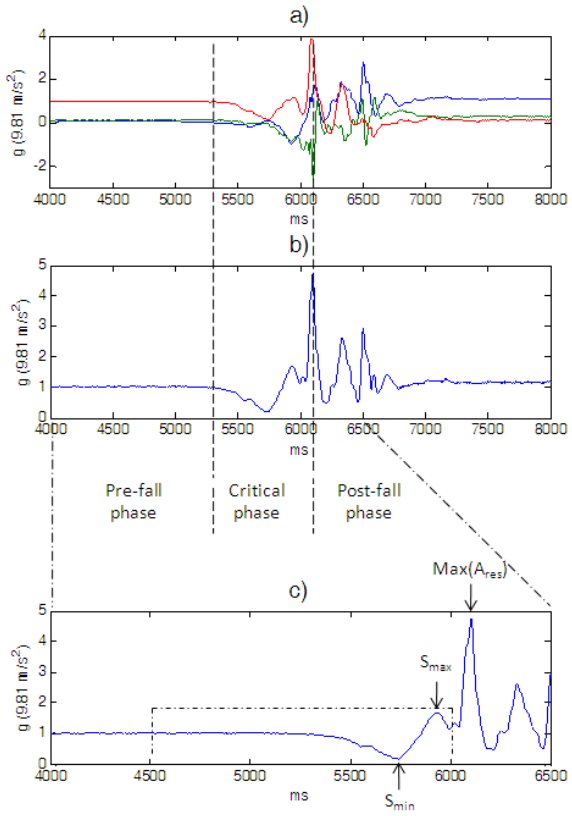

Figure 2: a) Example of general 3-axis acceleration for a left side fall. b) Example of the resultant acceleration corresponding to 2a. c) Part of the resultant acceleration including the critical phase signal of 2b. This part shows an example of 1.5 s sliding window, $S_{\min}$, $S_{\max}$, and $\max(A_{res})$.

Short time min-max feature

The short time min-max feature is separated from our previous algorithm [18]. High negative and positive peak resultant accelerations in critical phase fall signals are used for fall detection. To obtain the feature, the resultant acceleration signal is processed using a 1.5 s sliding window with 50% overlap. The 1.5 s window covers the critical phase fall signal. For the segmentation of data in each window, maximum resultant acceleration of the segmented signal ($S_{\max}$) and minimum resultant acceleration of the segmented signal ($S_{\min}$) are computed. $S_{\min}$ and $S_{\max}$ for a 1.5 s sliding window act as a short time min-max feature. An example of a sliding window, $S_{\min}$, and $S_{\max}$ are shown in Figure 2c.

D. Support Vector Machines

A Support Vector Machines (SVM) was employed as the classifier to separate falls from ADL [19]. It is composed of either an input for $\max(A_{res})$ or two inputs for $S_{\min}$ and $S_{\max}$. Three tested kernel functions follow: linear, polynomial with a default order of 3, and radial basis function (rbf) with a default scaling factor of 1. Data are normalized for training and testing. $\max(A_{res})$ of all the sequences, and $S_{\min}$ and $S_{\max}$ of all the segments of all the sequences, were divided into two groups for training and testing. The groups depended on the subjects, with balanced scenarios:

1) 7 sets of young/elderly subjects were numbered 1-7,
2) 7 sets of young/elderly subjects were numbered 8-14.

During training, the $\max(A_{res})$ for falls are set to fall events, while others are set to non-fall events for the maximum peak feature. For the short time min-max feature, only segments involving critical phase of falls for $S_{\min}$ and $S_{\max}$ are set to fall events, while others are set to non-fall events. Outputs (for the maximum peak feature) or segment outputs (for the short time min-max feature), which are greater than 0 denote falls. Otherwise, they are labeled as non-falls. Training and testing data were swapped for two-fold cross-validation.

E. Performance Evaluation

The performance is evaluated by sensitivity and specificity given by (2) and (3)

$$Sensitivity(\%) = \frac{TP}{TP+FN}*100 \qquad (2)$$

$$Specificity(\%) = \frac{TN}{TN+FP}*100 \qquad (3)$$

where TP (true positive): a fall occurs, the algorithm detects it; FP (false positive): the algorithm announces a fall, but it did not occur; TN (true negative): a normal (no fall) movement is performed, the algorithm does not declare a fall; FN (false negative): a fall occurs but the algorithm does not detect it. This event must be avoided because the elderly may receive serious injuries.

III. Results

A. Fall characteristics

An example of a left side fall acquired using a tri-axial accelerometer is illustrated in Figure 2. The left side fall is displayed in terms of x , y and z accelerations in Figure 2a. It is partitioned into three phases, a pre-fall phase, a critical phase, and a post-fall phase. In the pre-fall phase, or stand-still period, the z acceleration is about 1 g, while the x and y accelerations are about 0 g. As the body falls during the critical phase, there is a reduction of z acceleration below 1 g for a short period (or a high negative peak), and then increase until the body impacts the mattress with a high positive peak acceleration. In the post-fall phase, more than one peak usually occurs for several reasons, such as the knee impacting before the trunk for a forward fall, or the bottom impacting before the trunk in a backward fall, or due to rebounding of the body after impact. After impact, the acceleration direction reverses due to the rebound, and the body may impact/rebound several times until all the kinetic energy is exhausted. For the example, the z direction changes to be parallel with the ground and the y direction

switches to the vertical at the same time. At the end of a fall, the x and z accelerations are about 0 g while the y acceleration is about 1 g. Figure 2b shows the resultant acceleration for all the axis accelerations in Figure 2a. The resultant acceleration is about 1 g during the pre-fall phase, then drops below 1 g for a short period (or a high negative peak), before increasing to a peak. Figure 2c shows a part of the resultant acceleration, including critical phase, with an example of a 1.5 s sliding window, $S_{\min}$, $S_{\max}$, and $\max(A_{res})$.

B. *Fall and ADL resultant accelerations*

Figure 3 shows examples of resultant accelerations for different fall signals. These specific signatures appear in the critical phase for all falls, i.e. forward fall, backward fall, left and right side falls. The high positive peaks of the resultant accelerations from falls are generally several times the gravitational acceleration, and higher than those for ADL resultant accelerations, except for soft impacts. Figure 4 shows examples of ADL resultant accelerations. Even though ADL resultant accelerations have positive and negative peaks like fall resultant accelerations, their peaks are lower. They are usually in the interval (0.75–2 g), except for quick movements.

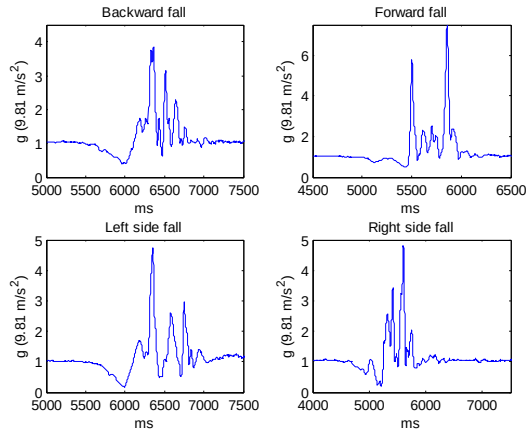

Figure 3: Example of resultant acceleration waveforms for different categories of fall.

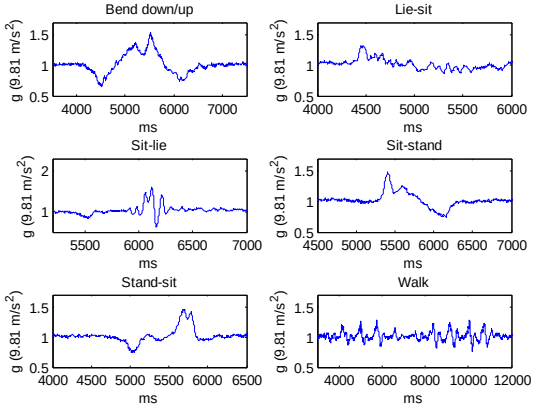

Figure 4: Example of resultant acceleration waveforms for different categories of ADL.

C. *Maximum peak feature*

The maximum peaks for the falls are usually greater than those for ADL for the first and second data groups as shown by quartile box plots in Figures 5a and 5b, respectively. Even though most falls are separate from ADL, several scenarios such as 'BF', 'LF', 'SL', and 'TS' have overlapping trend between falls and ADL using only a threshold.

For two-fold cross-validation with the SVM for each kernel, the first data group hyperplanes obtained from training were tested on the second data group, and the second data group hyperplanes were tested on the first data group. The sensitivities and specificities of each kernel for the maximum peak are shown in Table 1.

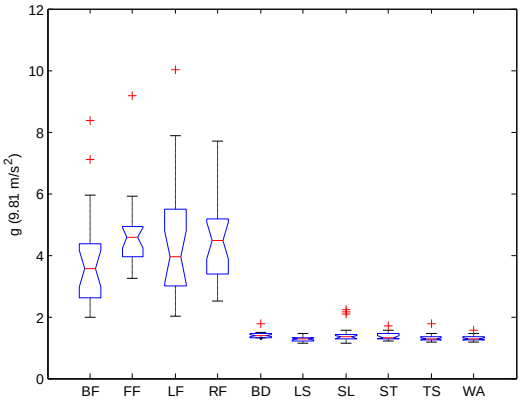

(a) First data group

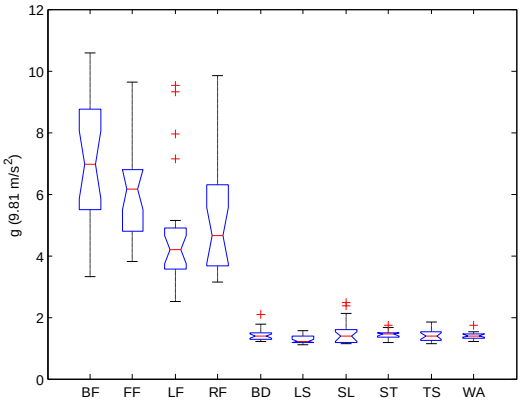

(b) Second data group

Figure 5: Quartile box plots of the maximum peak resultant accelerations of all sequences.

Kernel	Maximum peak	
	Sensitivity	Specificity
linear	91.1	99.2
polynomial	88.7	99.2
rbf	91.1	99.2

Table 1: Sensitivities and specificities for each kernel for the maximum peak.

Kernel	Short time min-max	
	Sensitivity	Specificity
linear	97.0	100.0
polynomial	95.2	100.0
rbf	98.2	100.0

Table 2: Sensitivities and specificities for each kernel for the short time min-max feature.

D. Short time min-max feature

Scatter plots of $S_{\min}$ and $S_{\max}$ of all sequences between critical phase fall and minimum before maximum ADL resultant acceleration for the first and second data groups are shown in Figure 6a and 6b, respectively. 'Red-o' symbols represent falls, while 'blue-x' symbols represent ADL. The $S_{\max}$ for the falls are usually greater than those for ADL, while $S_{\min}$ in the critical phase falls are usually lower than the minimum before maximum from ADL. These scatter plots show a trend for getting better rates of fall detection when the 1.5 s sliding window with 50% overlap slides among the critical phase fall.

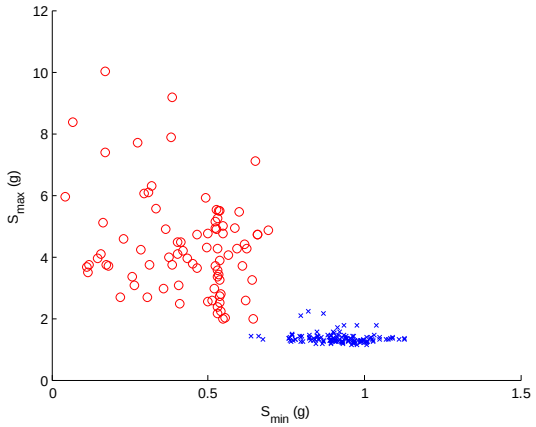

(a) First data group

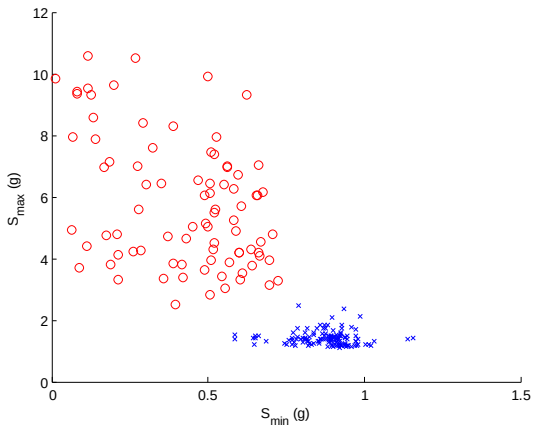

(b) Second data group

Figure 6: Scatter plots of $S_{\min}$ and $S_{\max}$ between critical phase fall and minimum before maximum ADL of all sequences.

For all segment data, most segment data for ADL have low $S_{\min}$ and $S_{\max}$. Segment data for non-critical phase falls have both low and high $S_{\min}$ / $S_{\max}$, because there are several changes of fall event influencing fall detection. For example, the pre-fall phase of a fall offers low $S_{\min}$ and $S_{\max}$ (about 1 g) and should be detected as a non-fall. The critical phase of a fall offers very low $S_{\min}$, which is usually lower than the minimum before maximum from ADL, and may offer high/maximum $S_{\max}$ depending on the reach of the sliding window to the maximum peak. Also, the post-fall phase, or the 'impacting and rebounding' period, may offer low/high $S_{\min}$ and $S_{\max}$ because of the alternative resultant acceleration. Therefore, the output segments of a fall sequence can be detected as a fall for segments of critical phase or some segments of post-fall phase, which have high negative and positive peaks like those from critical phase. These characteristics occur for segments involving critical phase before post-fall phase, so they are first detected in critical phase. However, if any segments of a fall sequence are predicted to be a fall, then the entire fall sequence is labeled as a fall.

Using the SVM for each kernel and two-fold cross-validation, the sensitivities and specificities of each kernel for the short time min-max are shown in Table 2.

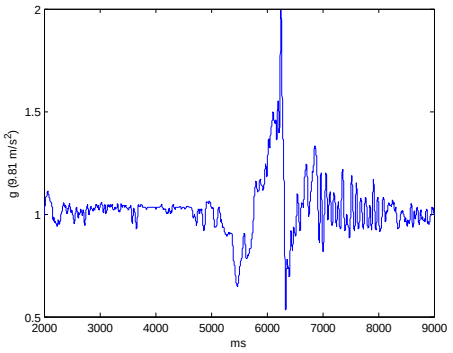

Figure 7: Resultant acceleration example of BF with false negative.

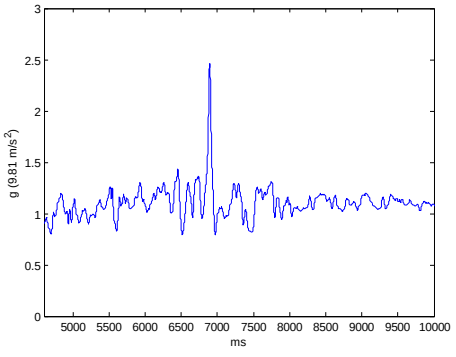

Figure 8: Resultant acceleration example of SL with false positive.

IV. Discussion

A number of BF produce FNs and a number of SL produce FPs for the maximum peak feature, as an example of BF and SL which produce FN and FP in Figures 7 and 8, respectively. The FN event of BF can be viewed as a body that sometimes impacts a mattress with acceleration lower than general, producing a soft impact, which gives a maximum peak like that from ADL. However, this case can be reduced by the short time min-max feature because the characteristic of minimum resultant acceleration in a critical phase can distinguish falls from ADL, as the results shown in Table 2. The FP event of SL can be described that a body sometimes impacts a mattress with acceleration greater than general, which produces a maximum peak like that from falls. This result is the same as in Chao' s study [13]. Although these cases of SL produce high maximum peaks, they do not produce high negative peaks for the elderly because of slow movement at a beginning of a descent onto a mattress. Thus, these cases of SL can be detected by the short time min-max feature. Chao' s study [13] shows that his method including AC- and PP-based algorithms, depending on a lying posture, cannot completely avoid FP. Our proposed method is not dependent on a posture after a fall, so it is a good choice for distinguishing SL from falls.

V. Conclusion

This paper presents a short time min-max feature for fall detection for the elderly. Our proposed feature employs the specific signatures of high negative and positive peak resultant acceleration in critical phase fall signals, to distinguish falls from ADL using a Support Vector Machine. The results show a performance comparison between the maximum peak and the short time min-max feature. For tests involving 420 sequences, we found that the sensitivities and specificities of short time min-max feature are greater than that of the maximum peak feature for all kernels. The kernel function of rbf offers the best performance for both features, which are 91.1% sensitivity and 99.2% specificity for the maximum peak feature and 98.2% sensitivity and 100% specificity for the short time min-max feature. The short time min-max feature gives better performance, uses only one sensor for a body's position, does not require a fixed threshold for 100% sensitivity or specificity, and does not involve additional processing for a posture after a fall. The simplicity and high performance of our proposed feature makes it suitable for implementation on a microcontroller for use in practical situations.

Acknowledgment

We are grateful to the Graduate School, Prince of Songkla University and the NECTEC-PSU Center of Excellence for Rehabilitation Engineering, for supporting this research. This work was also funded by a grant from NECTEC through Contract No P-00-10594.

References

[1] Nations (UN), *World Population Ageing 2009*, New York, USA., 2009.

[2] World Health Organization, *WHO global report on falls prevention in older age*, 2008.

[3] D. Carey, M. Laffoy, "Hospitalisations due to falls in older persons", *Irish Medical Journal*, 2005, vol. 98(6), pp. 179-181.

[4] B. S. Roudsari, B. E. Ebel, P. S. Corso, N. A. Molinari, T. D. Koepsell, "The acute medical care costs of fall-related injuries among the U.S. older adults", *Injury*, 2005, vol. 36(11), pp. 1316-1322.

[5] N. Noury, P. Rumeau, A. K. Bourke, G. ÓLaighin, J. E. Lundy, "A proposal for the classification and evaluation of fall detectors", *IRBM*, 2008, vol. 29(6), pp. 340-349.

[6] C. L. Huang, E. L. Chen, P. C. Chung, "Fall detection using modular neural networks with back-projected optical flow", *Biomed. Eng. Appl. Basis. Comm.*, 2007, vol. 19(6), pp. 415-424.

[7] M. N. Nyan, F. E. H. Tay, M. Z. E. Mah, "Application of motion analysis system in pre-impact fall detection", *J. Biomech.*, 2008, vol. 41, pp. 2297-2304.

[8] H. J. Lee, L. S. Chou, "Balance control during stair negotiation in older adults", *J. Biomech.*, 2007, vol. 40, pp. 2530-2536.

[9] D. T. H. Lai, R. K. Begg, S. Taylor, M. Palaniswami, "Detection of tripping gait patterns in the elderly using autoregressive features and support vector machines", *J. Biomech.*, 2008, vol. 41, pp. 1762-1772.

[10] C. S. Lin, H. C. Hsu, Y. L. Lay, C. C. Chiu, C. S. Chao, "Wearable device for real-time monitoring of human falls", Measurement., 2007, vol. 40, pp. 831-840.

[11] M. Kangas, A. Konttila, P. Lindgren, I. Winblad, T. Jämsä, "A comparison of low-complexity fall detection algorithms for body attached accelerometers", *Gait. Posture.*, 2008, vol. 28(2), pp. 285-291.

[12] M. Kangas, I. Vikman, J. Wiklander, P. Lindgren, L. Nyberg, T. Jämsä, "Sensitivity and specificity of fall detection in people aged 40 years and over", *Gait. Posture.*, 2009, vol. 29(4), pp. 571-574.

[13] P. Chao, H. Chan, F. Tang, Y. Chen, M. Wong, "A comparison of automatic fall detection by the cross-product and magnitude of tri-axial acceleration", *Physiol. Meas.*, 2009, vol. 30, pp. 1027-1037.

[14] A. K. Bourke, G. M. Lyons, "A threshold-based fall-detection algorithm using a bi-axial gyroscope sensor", *Med. Eng. Phys.*, 2008, vol. 30, pp. 84-90.

[15] A. K. Bourke, J. V. O'Brien, G. M. Lyons, "Evaluation of a threshold-based tri-axial accelerometer fall detection algorithm", *Gait. Posture.*, 2007, vol. 26, pp. 194-199.

[16] A. K. Bourke, P. Van de Ven, M. Gamble, R. O'Connor, K. Murphy, E. Bogan, E. McQuade, P. Finucane, G. ÓLaighin, J. Nelson, "Evaluation of waist-mounted tri-axial accelerometer based fall-detection algorithms during scripted and continuous unscripted activities", *J. Biomech.*, 2010, vol. 43(15), pp. 3051-3057.

[17] P. Jantaraprim, P. Phukpattaranont, C. Limsakul, B. Wongkittisuksa, "Evaluation of Fall Detection for the Elderly on a Variety of Subject Groups", *i-CREATe2009*, 2009, pp. 42–45.

[18] P. Jantaraprim, P. Phukpattaranont, C. Limsakul, B. Wongkittisuksa, "Improving the Accuracy of a Fall Detection Algorithm Using Free Fall Characteristics", *ECTI-CON2010*, 2010, pp. 530–533.

[19] T. Joachims, SVMlight: Support Vector Machine, [Online]. Available: http://svmlight.joachims.org/

Patimakorn Jantaraprim received the B. Eng. and M. Eng. degrees in electrical engineering from Prince of Songkla University, Thailand, in 1996 and 2001, respectively. She is currently a Ph.D. candidate of electrical engineering at Prince of Songkla University. Her research interests are signal processing and biomedical signal processing.

Pornchai Phukpattaranont was born in Songkla, Thailand. He received the B. Eng. and M. Eng. degrees in electrical engineering from Prince of Songkla University in 1993 and 1997, respectively, the Ph.D. degree in electrical engineering from the University of Minnesota, in 2004. He is currently an assistant professor of electrical engineering at Prince of Songkla University. His research interests are ultrasound contrast imaging, ultrasound signal processing, medical image processing, and biomedical signal processing. Dr. Phukpattaranont is a member of the IEEE.

Chusak Limsakul received D. Ing. in Electronics from Institute National des Sciences Appliquees de Toulouse, France, in 1985. D.E.A from Institute National des Sciences Appliquees de Toulouse, France, in 1982. B.Eng. degree in electrical engineering from King Mongkut's Institute of Technology Ladkrabang, Thailand, in 1978. In 1978 he joined Prince of Songkla University, Thailand as a lecturer in the

Department of Electrical Engineering. He is currently working as an Associate Professor in the Department of Electrical Engineering and Vice President for Research and Graduate studies at Prince of Songkla University, Thailand. His research interests are biomedical signal processing, biomedical instrumentation and neural network. He has contributed around 60 technical papers in various journals and conferences.

BooncharoenWongkittisuksa received the B. Eng. degree in electrical engineering from King Mongkut's Institute of Technology Ladkrabang, Thailand, in 1981, M. Sci. degree in biomedical instrumentation from Mahidol university, Thailand, in 1986. He is currently as an Associate Professor of electrical engineering at Prince of Songkla University. His research interests are electronics and biomedical instrumentation.